Science of the Total Environment 778 (2021) 146196

Contents lists available at ScienceDirect

Science of the Total Environment

journal homepage: www.elsevier.com/locate/scitotenv

Impacts of underground climate change on urban geothermal potential: Lessons learnt from a case study in London

Asal Bidarmaghz [a,*], Ruchi Choudhary [b,c], Guillermo Narsilio [d], Kenichi Soga [e]

[a] School of Civil and Environmental Engineering, University of New South Wales, Sydney, Australia
[b] Department of Engineering, University of Cambridge, Trumpington Street, CB2 1PZ, UK
[c] Data-centric Engineering, Alan Turing Institute, UK
[d] Department of Infrastructure Engineering, University of Melbourne, Parkville, Australia
[e] Department of Civil and Environmental Engineering, University of California, Berkeley, USA

HIGHLIGHTS

- A modelling framework for assessing geothermal potential in urban scale is shown.
- 12,700 BHEs, 13,300 basements and 15 km train tunnels are incorporated into the model.
- Geothermal extraction efficiency is impacted by ground conditions in permeable soil.
- Underground heated spaces contribute to geothermal potential in impermeable soil.
- Geothermal energy can support 50–75% of district's total gas demand.

GRAPHICAL ABSTRACT

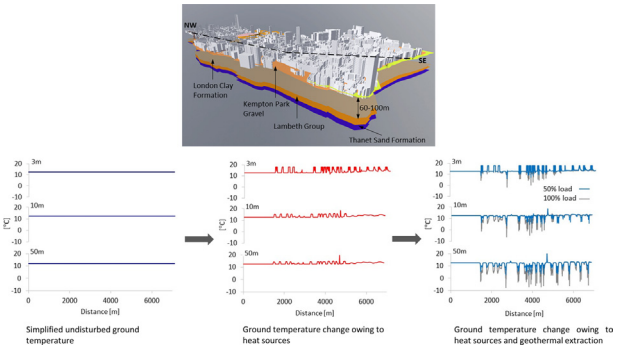

ARTICLE INFO

Article history:
Received 15 December 2020
Received in revised form 11 February 2021
Accepted 24 February 2021
Available online 6 March 2021

Editor: Jurgen Mahlknecht

Keywords:
Geothermal potential
Subsurface temperature
Underground climate change
Large-scale numerical modelling
Borehole heat exchangers
Subsurface urban heat island

ABSTRACT

While urban underground is being increasingly used for various purposes, two concerns should be addressed with respect to the urban underground climate change: i) how much energy has been stored in urban subsurface due to the heat rejection from underground heated spaces (such as tunnels and basements) and ii) how much of the thermal demand of a city or district can be supplied by harvesting this accumulative thermal energy in the ground. However, our understanding of the temperature rise in the ground and of the geothermal potential of urban subsurface is still limited. This paper quantifies the geothermal potential for a 12 km^2 densely populated borough in central London by considering the spatio-temporal temperature variation in the ground owing to continuous rejection of heat into the ground, coupled with the effect of geothermal extraction capacity. A large-scale transient semi-3D geothermal subsurface model of the site is developed, and the thermal interaction between underground heated spaces, geothermal energy extraction systems and the ground and groundwater are simulated. The concurrent heat rejection and extraction processes in the subsurface are computed so that the most influencing parameters of the subsurface on its geothermal potential are identified. Results show that up to 50% of the borough's total heat demand can be supplied via geothermal installations leading to around 33% reduction in CO_2 emission. The geothermal extraction efficiency in sand and gravel primarily depends on the ground conditions such as the thickness of the permeable layer and the groundwater flow regime. In impermeable ground such as clay, however, the underground built environment such as heated spaces have shown to have a significant impact on improving the geothermal extraction efficiency.

* Corresponding author.
E-mail address: a.bidarmaghz@unsw.edu.au (A. Bidarmaghz).

https://doi.org/10.1016/j.scitotenv.2021.146196
0048-9697/

1. Introduction

Past research has demonstrated that urbanisation has affected the shallow subsurface temperatures. A study by Ferguson and Woodbury (2004) was one of the first to examine the influence of heat flux from buildings to the ground in Winnipeg, Canada. It showed the extension of the ground temperature anomaly to be ~130 m vertically and 50 m laterally outward from a heated building, with a temperature increase of over 2 °C in 100 years. The combined effects of urbanisation and climate change on groundwater systems at a city-scale were investigated by Taniguchi et al. (2009). They concluded that subsurface temperatures of many urban areas are altered by surface warming and the heat island effect of urbanisation. More recently, as district-scale studies, a significant ground temperature rise in a densely populated district in London was shown to be induced by the heat rejected from residential basements and train tunnels to the ground (Bidarmaghz et al., 2019; Bidarmaghz et al., 2020).

The rise in underground temperature can potentially influence the resilience and efficiency of geothermal energy utilisation as urban geothermal potential is highly dependent on subsurface temperatures. Recent advances in urban subsurface temperature mapping through experimental monitoring and numerical simulations have contributed to assessing the viability of urban geothermal exploitation. For example, Allen et al. (2003) demonstrated that the temperature elevation of the high yielding urban aquifers with up to 4 °C temperature increase could fulfil the heating demand of buildings with a total footprint over 12,000 m^2. The work by Rivera et al. (2017) concluded that, for central Europe conditions, each additional degree of urban ground temperature could save around 4 m of the borehole length for the same heating power supply in Ground Source Heat Pump (GSHP) systems. Arola and Korkka-Niemi (2014) demonstrated that anthropogenic heat fluxes, in particular from buildings, have elevated groundwater temperature by about 3 to 4 °C in the city centre of the studied area. Therefore, it was concluded that approximately 50–60% more peak heating power could be utilised from populated areas compared with rural areas.

In addition to the above examples, the district- or city-scale contribution of geothermal systems (such as GSHPs) to the city's energy demand has been investigated by several researchers, for which a comprehensive review can be found in Bayer et al. (2019). Anderson and Rezaie (2019) presented several methods of harnessing energy through various geothermal technologies, whereas Østergaard and Lund (2011) demonstrated the advantages of the use of geothermal energy in combination with an absorption heat pump in a city in Denmark with the ultimate goal of becoming a 100% renewable energy city. Ondreka et al. (2007) developed an underground geothermal model for two study areas in south-western Germany with different geological settings using a geographic information system (GIS). In this model, the subsurface was divided into layers with similar thermal properties based on hydro-geological and lithological information. These maps were used to highlight the link between the heat extraction potential and ground conditions. A more detailed city-scale GIS-based simulation model was developed by Zhang et al. (2014) to estimate the number of geothermal installations at the city-scale without losing control of the ground thermal balance and to evaluate the degree to which such a system could contribute to the energy demands of buildings in a city. Epting et al. (2017) investigated the thermal state of groundwater in the cities of Basel, Switzerland and Zaragoza, Spain accounting for different hydraulic and thermal boundary conditions and assessed the anthropogenic thermal changes in the urban groundwater bodies. This assessment was used to facilitate planning for future aquifer use and urbanisation and to evaluate the thermal use potential of groundwater. Remediation strategies were defined for groundwater temperature control in which injection and extraction locations were considered where groundwater temperatures were elevated above 3 °C. In a similar study, Epting et al. (2018) assessed the temperature elevation and geothermal potential of urban groundwater in the city of Basel, Switzerland and compared it against the city's heat demand by relating the aquifer's temperature increase to the energy demand.

The impacts of ground temperature variations on geothermal systems have been studied at local and city-scales in recent literature, highlighting the profound thermal interaction between the geothermal systems and the subsurface (Barla and Di Donna, 2018; Bidarmaghz and Narsilio, 2018; Bidarmaghz et al., 2017; Cousin et al., 2018). For example, Epting et al. (2020) developed a multi-scale modelling approach where the thermal activation of the segmental lining was simulated using local-scale 3D thermo-hydro models. The results were used as transient boundary conditions to investigate the geothermal potential of the ground surrounding tunnel infrastructures in Basel, Switzerland. Applying a 3D finite element model, Bidarmaghz and Narsilio (2018) investigated the thermal interaction between energy tunnels, tunnel air, and the ground, highlighting the importance of groundwater regime on the efficiency of energy tunnels. Vienken et al. (2019) and Meng et al. (2019) investigated the impacts of shallow geothermal energy extraction on groundwater temperature in a 0.1 km^2 test area in the city of Cologne, Germany via an intensive temperature monitoring program and by using calibrated numerical models. Results showed that, despite the small energy demand and energy extraction rate in a relatively small study area (0.1 km^2), the accumulation of geothermal users significantly impacted the groundwater temperature.

The above-mentioned studies provide evidence that geothermal systems' long-term performance – particularly in urban areas – is significantly influenced by evolving subsurface infrastructure and underground climate. A key point is that the urban subsurface temperature is not uniformly elevated and is subject to both spatial and time variations resulting from a confluence of the distribution of heat sources and the ground's hydro-geological makeup. Yet, these effects are poorly understood at urban scales. As a result, the assessment of urban geothermal potential is often incorrect – especially with respect to long-term energy extraction efficiency (Radioti et al., 2017).

In most city-scale studies, the geothermal potential is evaluated by estimating a uniform and constant ground temperature rise over a fixed period in the subsurface and translating it to thermal energy by incorporating thermal properties of the ground (Allen et al., 2003; Arola and Korkka-Niemi, 2014). As such, there are no examples of evaluating the urban geothermal potential by taking into account the spatio-temporal variations of heat sources and hydro-geological ground properties.

This paper addresses this gap in the literature by presenting a large-scale finite element model of a dense urban district incorporating features of land surface cover, detailed hydro-geological properties of the ground, and anthropogenic heat sources, including 13,300 residential heated basements and 15 km of train tunnels. The spatio-temporal variation of ground temperature due to the simultaneous geothermal extraction and heat rejection from underground heat sources is the critical output influencing urban underground climate and hence sustainable exploitation of geothermal energy at the city-scale. The main novelty lies in quantifying the geothermal potential for an entire district (12 km^2) using a high resolution large-scale (appropriate urban catchment scale) geothermal model. The model accounts for the spatio-temporal temperature variation in the ground resulting from continuous heat rejection from underground heated structures, coupled with the effects of geothermal installations, ground conditions and groundwater regime. Up to now, in large-scale studies, this phenomenon is mostly overlooked by i) the simplified assumption of steady and homogenous ground temperature rise due to anthropogenic fluxes representing one-off heat contribution from underground heat sources to the ground or by ii) limited numbers of geothermal installations and/or underground heat sources, which yields rather a localised geothermal potential evaluation.

The numerical modelling approach presented in this study can be applied to any region to evaluate the geothermal potential of the

subsurface upon detailed knowledge of the ground and underground built environment characteristics.

2. The numerical model of urban-scale geothermal potential

The previous work of Bidarmaghz et al. (2020) investigated the ground temperature disturbance due to heat rejection from residential basements and train tunnels across a 12 km^2 district in central London. Temperature increases were observed in the subsurface, the magnitude of which varied spatially based on ground conditions and the distribution of underground heat sources. Considering the substantial temperature increase and heat accumulation in the subsurface, this paper evaluates the geothermal potential of the district by introducing a sufficient number of borehole heat exchangers into the subsurface to extract the accumulative heat. To do so, 12,700 heat sinks (as vertical borehole heat exchangers-BHEs) are added to the semi-3D finite element model introduced and detailed in Bidarmaghz et al. (2020) to evaluate the geothermal potential in the borough while considering the thermal effects of 13,300 basements and 15 km of train tunnels. It should be noted that a simplified outline has replaced the detailed outline of basements to avoid geometry irregularity, causing meshing expense. However, the simplification is undertaken such that the total basement area is kept consistent and the location and direction of the simplified basements are as close to the realistic basements footprints to minimise any impacts arising from groundwater flow direction. This model will be referred to as the *semi-3D geothermal model* in this paper, in which a new extension is introduced to facilitate the incorporation of geothermal installations into the previously developed large-scale subsurface model.

The main methodological difference between the semi-3D subsurface model presented in Bidarmaghz et al. (2020) and the semi-3D geothermal model presented in this paper is the numerical challenges of incorporating 12,700 borehole heat exchangers to the latter without compromising the size and the level of details of the urban-scale subsurface model. The semi-3D geothermal model takes into account the spatial non-homogeneity and time-dependency of temperature variation due to continuous rejection of heat into the ground and heat extraction via borehole heat exchangers on geothermal potential, providing a modelling framework that enables urban geothermal potential quantification at large scales. The model application contributes to the sustainability and efficiency of geothermal energy extraction, which has mostly been underestimated due to the assumption of steady and homogenous ground temperature rise representing one-off heat contribution from underground heat sources to the ground.

2.1. Semi-3D geothermal model specification

Following the work of Bidarmaghz et al. (2020), the semi-3D geothermal model is developed by dividing the entire subsurface into several 2D horizontal planes representing the depths between the ground surface and up to 100 m below surface. Fig. 1a illustrates a schematic of the semi-3D model and the equivalent full 3D representative of the modelled area. Heat transfer and fluid flow at each horizontal plane (XY) are quantified. Heat transfer in the vertical direction Z (representing depth in the ground) is calculated by coupling the temperature distribution at each depth to the temperature distribution of a shallower depth and a deeper depth using Fourier's Law of heat conduction – applying selected vertical distance between the planes and the thermal properties. These plane intervals are selected based on the changes occurring in ground conditions and subsurface structures (e.g., at the top and bottom of basements and tunnels and at any depth in which soil properties change) to ensure that subsurface parameter variations (e.g., ground properties, structural geometry) are fully captured in this model. It should be noted that the hydraulic conductivity of different types of soils, in general, is smaller in the vertical direction than in the horizontal direction (i.e., $k_v/k_h = 0.1–0.5$, (Todd, 1959)). Therefore, by selecting plane intervals that capture all the depth-dependent variations in the model, the impact of neglecting the vertical mass transfer between the planes on the model outputs can be minimised to an acceptable level (details can be found in Bidarmaghz et al. (2020)).

The borehole heat exchangers are represented as point heat sinks at each plane to enable heat extraction from the ground. Point sinks are activated in planes from the surface to 50 m below the ground surface. They are thermally coupled to one another in the vertical direction to represent a borehole heat exchanger with a typical length of 50 m. Basements are activated in planes from the surface to 3 m below the ground surface (typical depth for basements on London (RBKC, 2018)) and train tunnels being activated in the relevant planes based on their depth. While the spatial distribution of basements and train tunnels were extracted from geo-mapping datasets (GeoInformation, 2017a; GeoInformation, 2017b; RBKC, 2018), the borehole heat exchangers are evenly distributed in the vicinity of buildings with 10 m distance between the heat exchangers (Kavanaugh and Rafferty, 2014). No geothermal installation is considered for areas within which train tunnels are in the first 50 m below the subsurface. A typical 2D plane at any given depth comprising residential basements, train lines (tunnels) and, point heat sinks is shown in Fig. 1b.

Detailed local subsurface geology, hydrogeology, and the district's ground thermal properties are derived from a 3D geological and groundwater model developed by the British Geological Survey (BGS) (British Geological Survey, 2017) and are incorporated into the semi-3D geothermal model. Fig. 2a shows the geological model and its variations along a NW-SE section, showing relatively consistent geological units of the area predominantly varying between River Terrace Deposits (various types of gravel) up to 10 m below the surface and London Clay Formation (up to 60–100 m below the surface).

The estimated values of thermal conductivity and diffusivity for River Terrace Deposits and London Clay Formation are shown in Table 1 (Bricker and Bloomfield, 2014; British Geological Survey, 2017; Busby et al., 2009). The ground thermal properties for different geological units (mostly gathered from Thermal Response Testing results around the UK) are spatially integrated into the model. The distribution of the selected thermal conductivity, heat capacity and thermal diffusivity, reflects the typical thermal properties of the geological units in the borough, which vary between River Terrace Deposits (e.g., Kempton Park Gravel) and London Clay Formation. The hydraulic conductivities for River Terrace Deposits are from a conceptual model developed by British Geological Survey (Burke et al., 2014) across the Thames Basin for different lithostratigraphic classes of superficial deposits including River Terrace Deposits (saturated and unsaturated). The hydraulic conductivity for London Clay Formation is extracted from the literature (Busby et al., 2009). The overall groundwater level distribution based on observation well measurements is shown in Fig. 2b-left. For the southern part of the borough within which up to 10 m below the surface could consist of permeable River Terrace Deposits, The British Geological Survey provided an updated hydraulic head distribution based on the shallow groundwater levels and by taking into account the lost rivers of Fleet and Westbourne and the River Thames - with a long-term average recharge rate of 0.12 m/day, and accounting for rainfall and potential evaporation in the area. This is shown in Fig. 2b-right (Mansour and Hughes, 2004; Mansour et al., 2018).

The total thermal demand of a typical residential building in this district of London (attached terrace houses according to GeoInformation (2017a)) is specified as average gas consumption of 12,500 kWh per household for space heating and hot water (Choudhary, 2012). As water heating relies on both electric and gas, its contribution to the annual average consumption deems minimal. Therefore, according to Zimmermann et al. (2012), the gas consumption of a typical household in London can vary between the extreme cases of three times higher than the average value (in winter) and zero (in summer), leading to the annual thermal load profile presented in Fig. 3. A typical value of

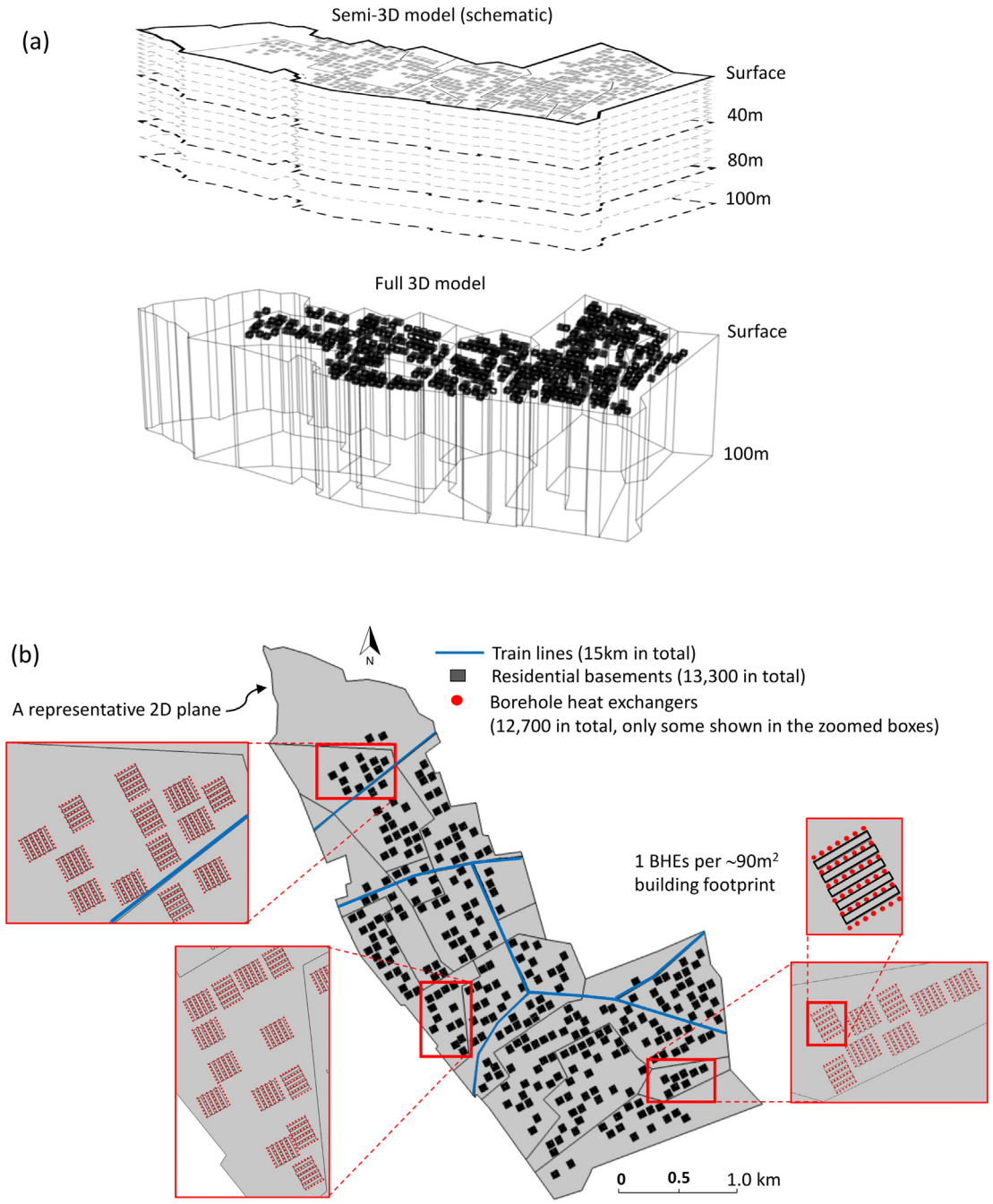

Fig. 1. Geothermal model (a) schematic of the semi-3D model and the 3D representative of the modelled area (not to scale), (b) a 2D plane representing residential basements, train lines and point heat sinks (BHEs).

30 W/m was selected as the average geothermal extraction rate (Banks, 2012; Bidarmaghz et al., 2015; Johnston et al., 2011). Given the largely heating dominated case, the relatively small heat rejection into the ground via the BHEs during the warmer weeks of summer is not considered in this study, making the study rather conservative. The geothermal extraction rate's annual variation follows the same trend as the thermal demand leading to the maximum heat extraction rate of ~80 W/m in winter and zero in summer (presented in Fig. 3, secondary vertical axis).

Considering the average gas consumption per household, the number of buildings and the average geothermal extraction rate (30 W/m), 12,700 ground heat exchangers of 50 m in length will be required to ideally supply the total thermal demand of the borough. However, ground freezing due to heat extraction is the prohibitive factor, which defines the ultimate geothermal potential in the subsurface. Therefore, to evaluate the maximum heat extraction capacity of the ground (which can also be translated as the supply of a thermal demand which does not result in ground freezing), thermal load intensities of 100%, 75% and 50% of the total thermal demand of the district are modelled, and the consequent ground temperature decreases are quantified. Furthermore, the impact of heated basements on the geothermal potential is quantified by neglecting the heat rejection from basements in one model run, while heat extraction via borehole heat exchangers continued. The outputs are compared to the case where basements act as heat sources by rejecting heat to the ground, thus thermally interacting with the borehole heat exchangers.

Heat exchange between the basements, train lines, borehole heat exchangers and the surrounding ground and groundwater at each 2D

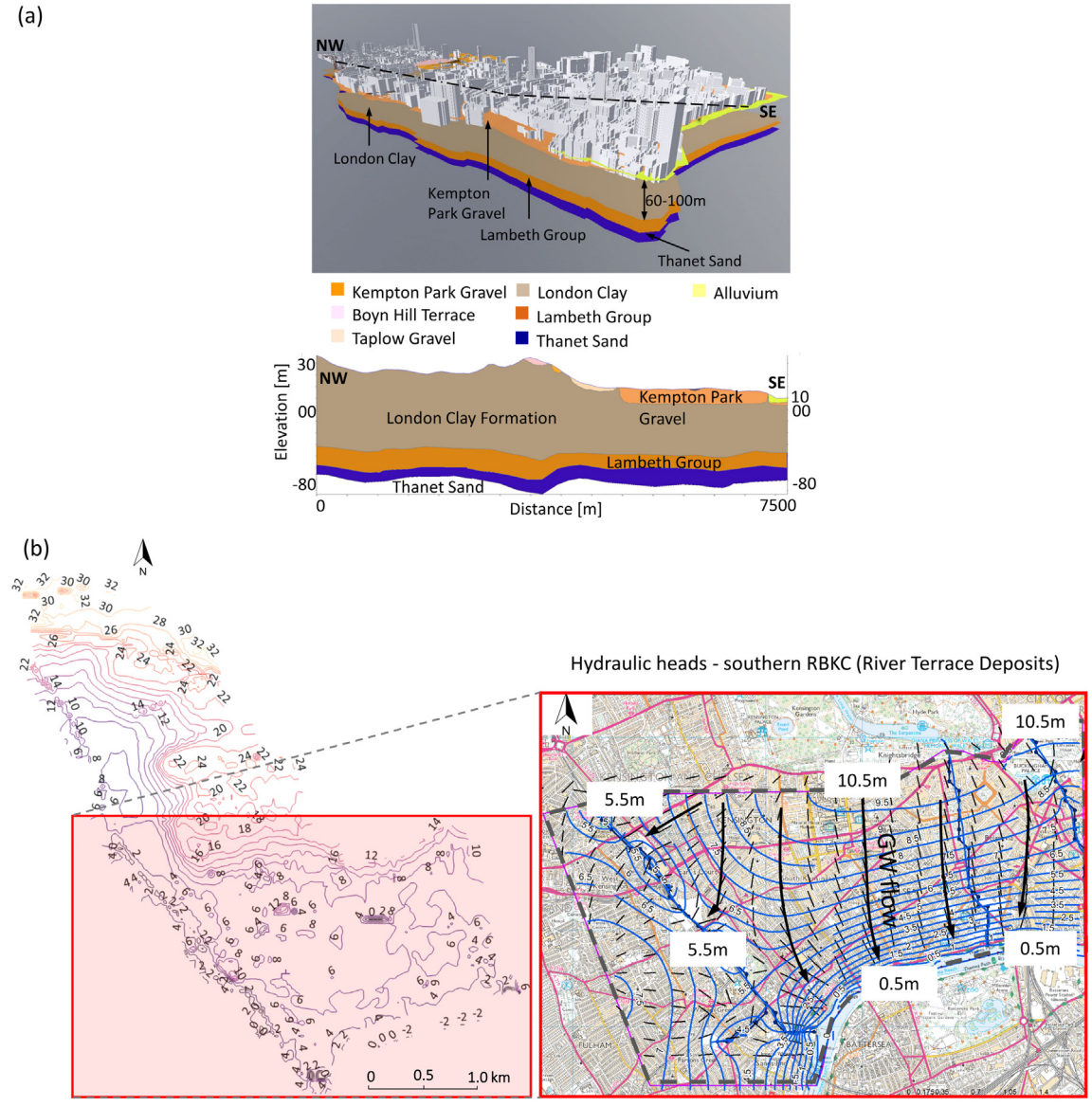

Fig. 2. (a) 3D Geological model and geological variations, (b) groundwater level contours (relative to Ordnance Datum) and estimated hydraulic heads (Bidarmaghz et al., 2020).

plane is captured by coupling and solving the equations for conductive and convective heat transfer and fluid flow in a porous medium (ground) with groundwater flow (Eqs. (1)–(4)) using finite element package COMSOL Multiphysics (Bidarmaghz, 2014; COMSOL, 2018a; COMSOL, 2018b). It is worth noting that the following equations were initially developed in the work of Bidarmaghz et al. (2020); however, they are presented in this work to show the modifications for heat sinks' incorporations:

$$d_z(\rho Cp)_{eff}\frac{\partial T}{\partial t} + d_z(\rho Cp)\mathbf{v_f}.\nabla T + \nabla.q = q_{0,up} + q_{0,down} + Q_{applied}d_z \quad (1)$$

$$q_{0,up} = \lambda_{eff}(T_{n-1} - T_n)/dz \text{ and } q_{0,down} = \lambda_{eff}(T_{n+1} - T_n)/dz \quad (2)$$

$$q = -d_z\lambda_{eff}\nabla T \quad (3)$$

$$\lambda_{eff} = (1-\varepsilon)\lambda_m + \varepsilon\lambda_f \quad (4)$$

where d_z is the distance between the planes (domain thickness) [m], $(\rho C_p)_{eff}$ is the effective density [kg/m^3] and effective heat capacity [J/kgK] of the porous ground, v_f is the Darcy velocity field [m/s] - in the presence of groundwater, λ_{eff} is the effective thermal conductivity of the porous ground [W/mK], λ_f and λ_m represent the thermal

Table 1
Hydro-thermal properties of the ground (RBKC) used in the semi-3D geothermal model.

Geology	Thermal conductivity, λ [W/(mK)]	Density, ρ [kg/m^3]	Specific heat capacity, C_p [J/(kgK)]	Porosity [−]	Hydraulic conductivity, k_h [m/s]	Diffusivity, α [m^2/s]
Kempton Park Gravel (unsaturated)	0.77	1600	1100	0.35	4.2×10^{-5}	4.5×10^{-7}
Kempton Park Gravel (saturated)	2.5	1900	1440	0.35	5.6×10^{-4}	9.1×10^{-7}
London Clay	1.7	2000	870	0.5	1×10^{-9}	9.7×10^{-7}

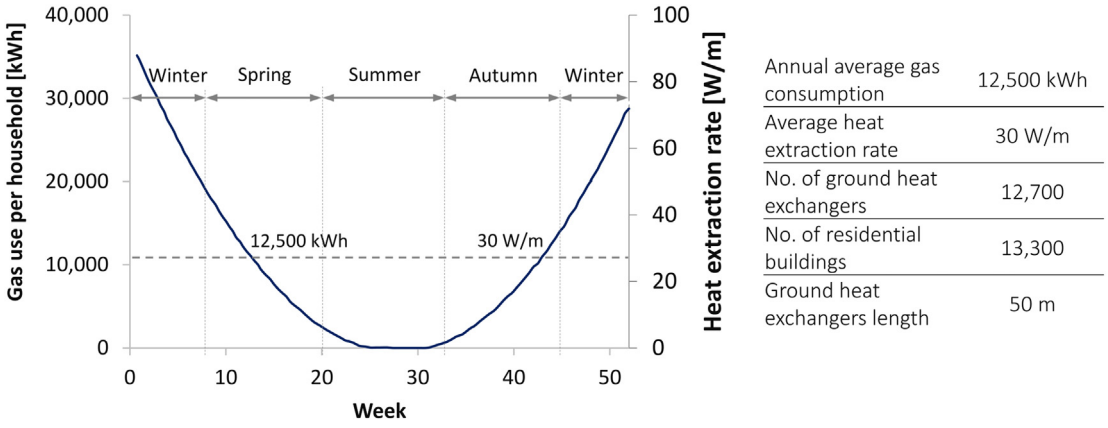

Annual average gas consumption	12,500 kWh
Average heat extraction rate	30 W/m
No. of ground heat exchangers	12,700
No. of residential buildings	13,300
Ground heat exchangers length	50 m

Fig. 3. Annual gas consumption for space heating and hot water for a typical household and the associated geothermal extraction rate.

conductivity of groundwater and solid material respectively [W/m.K] and ε is the porosity. T is the transient temperature [K], $q_{0,up}$ and $q_{0,down}$ are the upside and downside out of plane heat fluxes [W/m^2], which are used to account for heat transfer in the vertical direction Z (between the planes n, n-1 and $n+1$) based on the effective thermal conductivity between the planes and their temperature differences and $Q_{applied}$ is the thermal load applied at the point heat sinks at each plane [W/m] representing the vertical borehole heat exchangers by accounting for the vertical distance between the planes (dz).

Single-phase fluid flow in a porous medium (groundwater flow) is described by Darcy's Law as described in Eqs. (5) and (6)

$$\mathbf{v_f} = -\frac{K}{\mu_f}\left(\nabla p_f - \rho_f g \nabla Z\right) \quad \frac{K}{\mu_f} = \frac{k_h}{\rho_f \mathbf{g}} \tag{5}$$

Inserting Darcy equations into the continuity equations produces the generalised governing equation:

$$\frac{\partial}{\partial t}\left(\varepsilon \rho_f\right) + \nabla.\rho_f\left[-\frac{K}{\mu_f}\left(\nabla p_f - \rho_f \mathbf{g} \nabla Z\right)\right] = 0 \tag{6}$$

where K is the permeability of the ground [m^2/s], p_f represents the pore pressure in the ground [Pa], ρ_f is the temperature-dependent groundwater density [kg/m^3], g is the gravitational acceleration vector [m/s^2], μ_f is the groundwater dynamic viscosity [Pa·s] and $\mathscr{E}$ is the porosity.

It should be noted that the semi-3D geothermal model consists of one 2D plane only. However, several sets of heat transfer and fluid flow equations are defined, for which, each set of equations (with variables of temperature, T, pressure, p, and velocity, v) refer to one specific depth, taking into account the hydro-geology and underground built environment at that depth.

The initial and boundary conditions incorporated into the semi-3D geothermal model are presented in Fig. 4. Overall, the heat extraction rate applied at point sources varied seasonally and between 0 and ~80 W/m, as shown in Fig. 3 (Zimmermann et al., 2012). The existing groundwater flow rate and direction in the southern part of the district

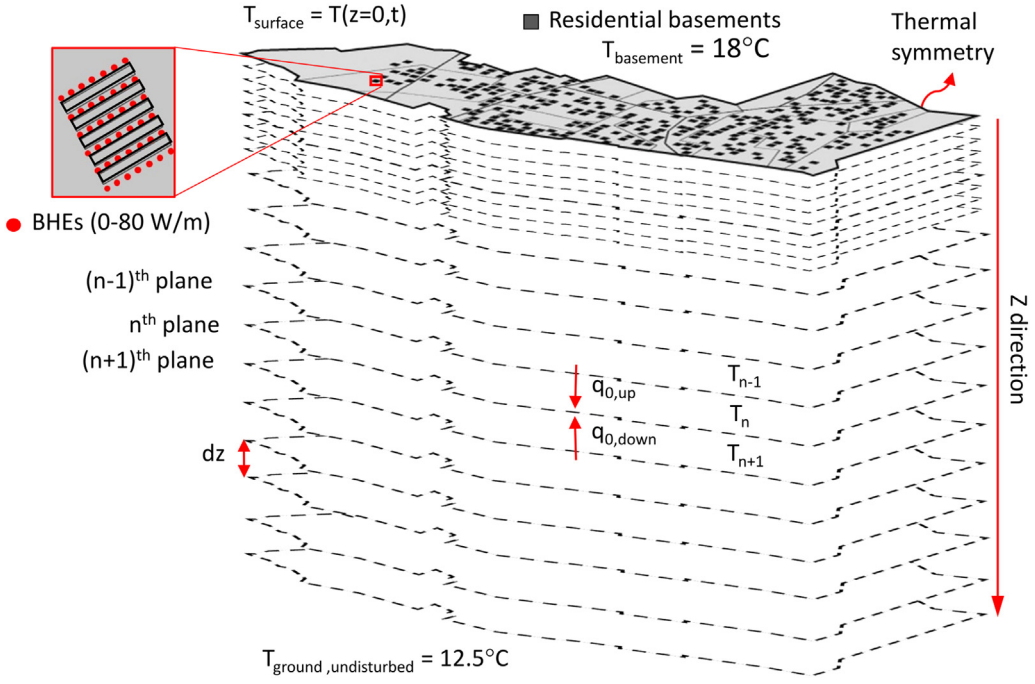

Fig. 4. Schematic of the initial and boundary conditions used in the semi-3D geothermal model.

(where permeable superficial deposits exist) are modelled by assigning the relevant hydraulic properties (i.e., hydraulic conductivity and hydraulic head distribution) to each plane. As shown in Fig. 2b, within southern parts of the district, the maximum head difference (relevant to Ordnance Datum) is around 10 m for the east boundary and 5 m for the west boundary of each plane within the first 10 m below ground level. The basements are kept at the average indoor temperature in the UK (18 °C) throughout the year (Lane, 2011; Menberg et al., 2016). Train line temperatures followed an annual temperature distribution that varies seasonally between 15 and 28 °C for London's typical conditions representing average annual temperature distribution for different train lines in London based on the temperature data presented in the works of Mortada (2019) and Gilbey et al. (2011). The outer boundary of the planes is set as symmetry, assuming similar thermal disturbance in the ground from basements and train lines within the neighbouring boroughs. The effect of ground surface temperature fluctuations is captured as a time-varying temperature. This surface temperature is accounted for in the first plane using Eq. (7) (Baggs, 1983; Bidarmaghz et al., 2016):

$$T_{surface}(z=0,t) = T_{ground,undisturbed} - (1.07.k_v.A_s \times \exp(-0.00031552.(z=0).\alpha^{-0.5}) \times \cos\left(\left(\frac{2\pi}{365}\right).(t - t_0 + 0.018335.(z=0).\alpha^{-0.5})\right) \quad (7)$$

where $T_{ground,undisturbed}$ is the ground annual average temperature (12.5 °C), k_v is the vegetation coefficient set at 0.8 accounting for an average of 30% vegetation cover, A_s is the annual air swing temperature (8.3 °C), t is the day of the year, z indicates the depth in the ground and equal to 0 for the ground surface [m], α is the ground diffusivity equal to an average value of 9.65×10^{-7} m^2/s calculated based on physical and thermal properties of the soil presented in Table 2 and t_0 is the coldest temperature day from January 1st (Busby et al., 2009; Price et al., 2018).

Each 2D plane consists of about 300,000 triangular elements. The model is executed on an Intel 2.1 GHz, 24 cores with 192 GB memory, co-simulating up to 34 planes (from the surface to about 100 m below surface), hence 34 sets of temperature, Darcy velocity and pressure variations. The total finite element model is ~100 GB in size.

2.2. Semi-3D geothermal model validation

The specification of the large-scale geothermal model requires validation, which is presented in this section. The ground temperature changes in the semi-3D model with point heat sinks at each horizontal plane are compared to the outputs from a validated 3D model (Bidarmaghz and Narsilio, 2016) comprising the ground as a 3D domain and a line heat sink as the vertical borehole heat exchanger (Fig. 5a). A constant heating demand of 50 W/m is applied on the heat sinks of both models (as a line in the 3D model and as points in the semi-3D model). The semi-3D model is divided into 11 planes with 1 m plane intervals, in which the point heat sinks are activated in the first 10 planes - to represent a 9 m long line source similar to the 3D model. Eq. (8) for steady-state conductive-convective heat transfer together with Eqs. (2)–(4) (presented in 2.1) are solved in the finite element package COMSOL Multiphysics to model heat transfer mechanism between the ground

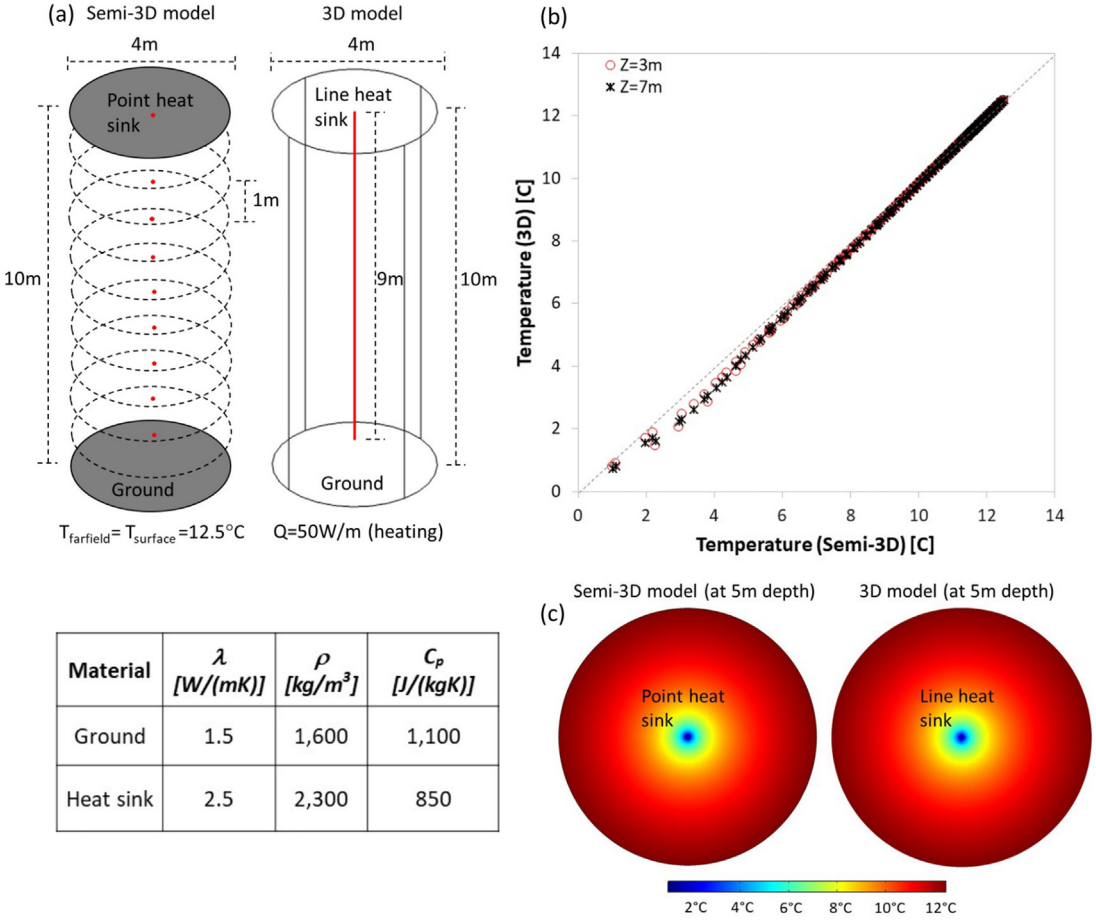

Material	λ [W/(mK)]	ρ [kg/m^3]	C_p [J/(kgK)]
Ground	1.5	1,600	1,100
Heat sink	2.5	2,300	850

Fig. 5. Model evaluation: (a) schematic of the 3D vs semi-3D models, (b) ground temperatures obtained from semi-3D and 3D models, (c) planar ground temperature distribution at mid-depth of semi-3D and 3D models.

and heat sinks (borehole heat exchangers) at each horizontal plane and in the vertical direction Z in the semi-3D geothermal model (Bidarmaghz, 2014; COMSOL, 2018a; COMSOL, 2018b):

$$d_z(\rho Cp)_{eff}\mathbf{v_f}.\nabla T + \nabla.q = q_{0,up} + q_{0,down} + Q_{applied}d_z \quad (8)$$

where d_z is the distance between the planes (domain thickness) [m], $(\rho C_p)_{eff}$ is the effective density [kg/m^3] and effective heat capacity [J/kgK] of the porous ground, v_f is the Darcy velocity field [m/s] - in the presence of groundwater, T is the temperature [K], $q_{0,up}$ and $q_{0,down}$ are the upside and downside out of plane heat fluxes [W/m^2], which are used to account for heat transfer in the vertical direction Z (between the planes n, n-1 and $n+1$) based on the effective thermal conductivity between the planes and their temperature differences and $Q_{applied}$ is the constant thermal load applied at the point heat sinks at each plane [W/m] representing the vertical borehole heat exchangers by accounting for the vertical distance between the planes (d_z).

It is noteworthy to mention that groundwater is not included in the validation model (groundwater and Darcy equations are fully incorporated into the large-scale semi-3D geothermal model explained in Section 2.1); therefore, the groundwater-related terms in the equations above ($\mathbf{v_f}$, λ_f *and* ε) are set at zero. Details of the full 3D finite element model can be found in Bidarmaghz and Narsilio (2016).

Temperature ranges obtained from the full 3D and semi-3D models at different depths are compared and presented in Fig. 5b and c. These observations indicate that the accumulative effect of point heat sinks in the semi-3D geothermal model is a reasonable representation of the line heat sinks in the full 3D model.

3. Results and discussions

The semi-3D geothermal model explained in Section 2.1 is used to study the thermal interaction between 13,300 heated residential basements, 15 km of train tunnels and 12,700 borehole heat exchangers and the ground. Accounting for hydro-geological variations, the geothermal exploitation efficiency in different parts of the borough is investigated with respect to the spatial variations of the ground temperature. To evaluate the optimal heat extraction capacity of the subsurface, several thermal demand intensities are tested (100%, 75% and 50% of the total gas consumption of the borough), for which the consequent ground temperature decrease is quantified. To do so, numerical simulations are conducted for a period of 25 years with the ground surface and train tunnel temperatures and heat extraction rate varying with time, while the temperature of the basement is kept at a comfortable level of 18 °C throughout the year.

Fig. 6a shows the spatial distribution of the subsurface temperature – after 25 years – when 100% of the borough's heat demand is supplied by geothermal energy. It should be noted that the temperature values presented in Fig. 6 are the minimum values occurring in the ground due to heat extraction (T_{min}), and $T_{min\text{-}initial}$ is the minimum ground temperature, mid-winter, prior to heat exchangers' activation. It is observed that the location of heat sources, the geological makeup and the groundwater regime result in large spatial variations in ground temperatures, thus the geothermal energy efficiency. For example, at 6 m depth, the activation of borehole heat exchangers within the London Clay Formation results in the ground temperature decreasing from 12.3 °C ($T_{min\text{-}initial}$) to a minimum of −15 °C (T_{min}). The minimum ground temperature is higher at shallower depths (e.g., −10.3 °C at 3 m) in this formation as a result of the continuous heat rejection from the basements. Conversely, the same thermal load has a negligible effect on the subsurface temperatures within the River Terrace Deposits, with groundwater flow (up to 10 m below surface) showing significantly higher ground temperatures in that area. At deeper depths (e.g., 36 m), where ground dominantly consists of London Clay, the thermal compensation from heated basements and train lines decreases while heat extraction via borehole heat exchangers is continuous. This results in an extreme minimum ground temperature in the entire borough, indicating the limitation of the geothermal system to fulfil 100% of the borough's heat demand.

To explicitly study the heated underground spaces' contribution to the efficiency of geothermal systems, heat rejection from basements is not included in model execution, while the borehole heat exchangers remain activated to supply 100% of the total thermal demand. Prior to the activation of heat exchangers, the minimum ground temperature in the borough was 11 °C within the seasonal fluctuation zone (up to 6 m depth) and around 12.5 °C at deeper depths. As shown in Fig. 6b, and as one would expect, the temperature of the ground reduces by the geothermal extraction. However, in comparison to the model where basements act as heat sources (shown in Fig. 6a), the ground temperature in shallow subsurface consisting of London Clay is significantly lower (−18.2 °C at 3 m and − 21.9 °C at 6 m). At deeper depths and in the areas of the borough with sand and gravel, the effect of heated basements on ground temperature seems to be minimal (3.6 °C vs 6.2 °C at 3 m and − 21.9 °C vs −22 °C at 36 m). These results indicate that the greatest benefits of the heated underground spaces for geothermal potential are achieved when these structures are in the impermeable ground (e.g., London Clay). Despite the positive effect of heat sources on geothermal potential, when located within permeable material, the groundwater flow is the primary phenomenon in improving the efficiency of geothermal energy extraction by preventing significant temperature decrease in the ground due to geothermal energy extraction.

The results shown in Fig. 6 indicate that the supply of the 100% thermal demand of the district via borehole heat exchangers is not viable due to substantial sub-zero temperatures occurring within the London Clay Formation. Therefore, thermal demand intensities of 75% and 50% of the total load are incorporated into the model to further understand the maximum geothermal energy extraction capacity of the subsurface. It is demonstrated that the permeability values of the ground and groundwater flow have favourable impacts on the geothermal potential. However, its extent varies by the thermal load intensity.

Fig. 7 shows the minimum ground temperatures (depth-averaged) taken from the volume of the ground with different permeable layer thicknesses - for thermal load scenarios of 100%, 75%, and 50% of total thermal demand. The minimum ground temperature of a case with no geothermal energy extraction (referred to as “No BHEs”) is also presented for comparison. It is observed that, were the ground consists of layers of permeable soil, the geothermal efficiency improves by yielding higher minimum ground temperatures. For example, where the thickness of the permeable layer is relatively large - areas in the borough where the first 10 m of the subsurface is covered with River Terrace Deposits – the minimum ground temperature shows less sensitivity to the variations of the thermal demand (between the range of −3.4 °C to 1.9 °C for 75% and 50% thermal load intensities). This is primarily due to the effect of groundwater flow in recharging the ground surrounding the borehole heat exchangers and is secondarily attributed to the impact of heated basements on geothermal efficiency in the permeable ground. Conversely, in areas where the London Clay Formation outcrops (0 m of the permeable layer), the minimum ground temperature range is large and varies between −9.1 °C to −1.6 °C for 75% and 50% thermal demand, showing significantly lower geothermal extraction efficiency for all thermal load intensities in such formation.

By comparing the minimum ground temperature for thermally insulated vs. thermally activated basements (for 100% load) for different thicknesses of sand and gravel in Fig. 7, it is concluded that the contribution of the heated basements to the geothermal extraction efficiency increases when the thickness of the permeable layer decreases. For example, for the 100% thermal load the activation of heated basements located in London Clay has increased the minimum ground temperature by around 4 °C (from −18.5 °C to −14.1 °C), which is about 1 °C (from −9.8 °C to −8.7 °C) in the ground with 10 m of permeable soil.

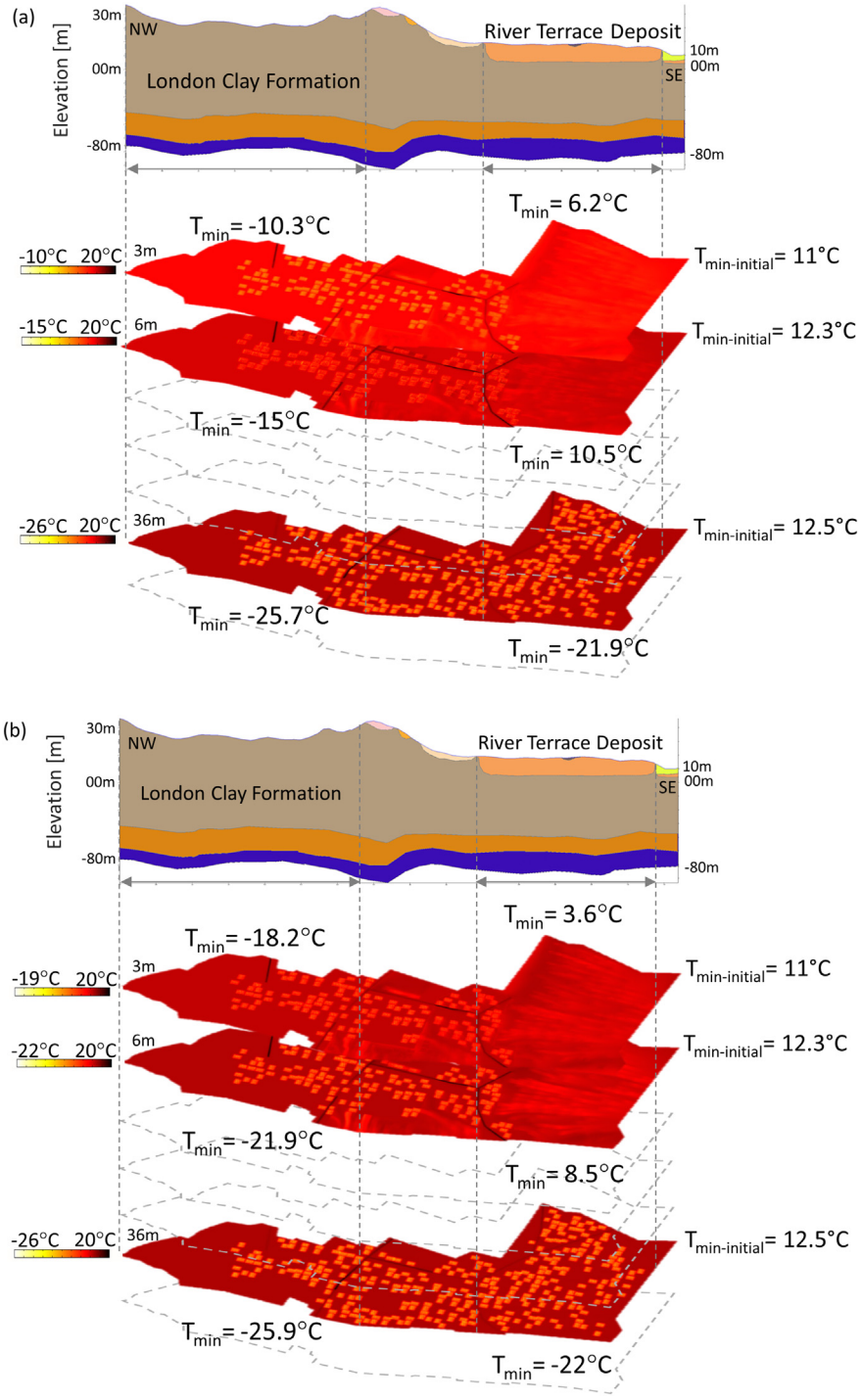

Fig. 6. Spatial variations of ground temperature due to fulfilling 100% of the district's thermal demand using borehole heat exchangers (a) with activated heated basements, (b) with thermally insulated basements. Note the different range scale at different depths.

These observations highlight the spatial dependency of geothermal extraction capacity. Therefore, a good understanding of the spatial temperature variations in the ground is crucial to ensure the efficiency of geothermal extraction. Fig. 8 shows the spatial variation of ground temperature for a NW-SE section of the borough due to the combined effect of heated basements, geological makeup and groundwater flow.

In parts of the district where the River Terrace Deposit outcrops, the effect of groundwater flow results in minimal ground temperature decrease at a depth of the basements (3 m) and the depth in which the ground is permeable and allows groundwater to flow. This, in turn, results in smaller differences in the ground temperature for different thermal load distributions (50% and 100%). The geothermal extraction efficiency is higher in such hydro-geological conditions, and also the geometrical characteristics of heated underground spaces (e.g., depth) can contribute to the geothermal potential of the urban subsurface in such geological makeup. In contrast, in the London Clay Formation, even though heated basements significantly increase the ground temperature surrounding the basements, the contribution is not enough

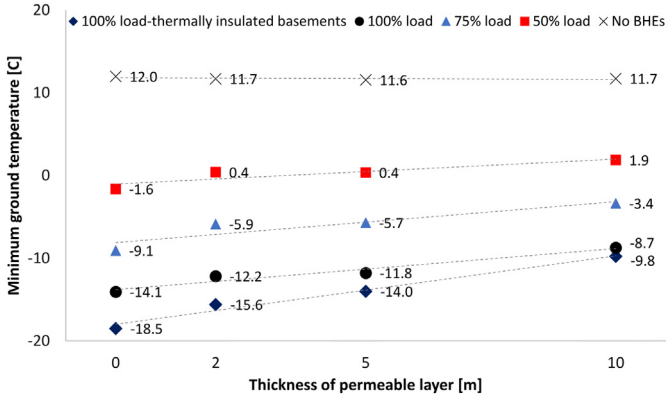

Fig. 7. Volumetric minimum ground temperature (depth-averaged) at different parts of the borough.

to avoid significant sub-zero temperatures in the ground due to geothermal extraction.

The heat extraction capacity is strongly correlated to the thermal load intensity – at any depth – and shows a significant variation in ground temperatures for different thermal loads (50% vs. 100%). Therefore, it can be concluded that in impermeable soil, even though heated basements have positive impacts on geothermal potential and higher minimum temperatures to occur in the ground (as shown in Fig. 6), the effect is not as profound as the combined effect of heated basements and groundwater flow in permeable soil. Ground thermal capacity, which is defined by thermal diffusivity, is the key parameter in urban geothermal potential evaluations in such impermeable formations. It should be noted that the sharp temperature increase at 4700 m distance

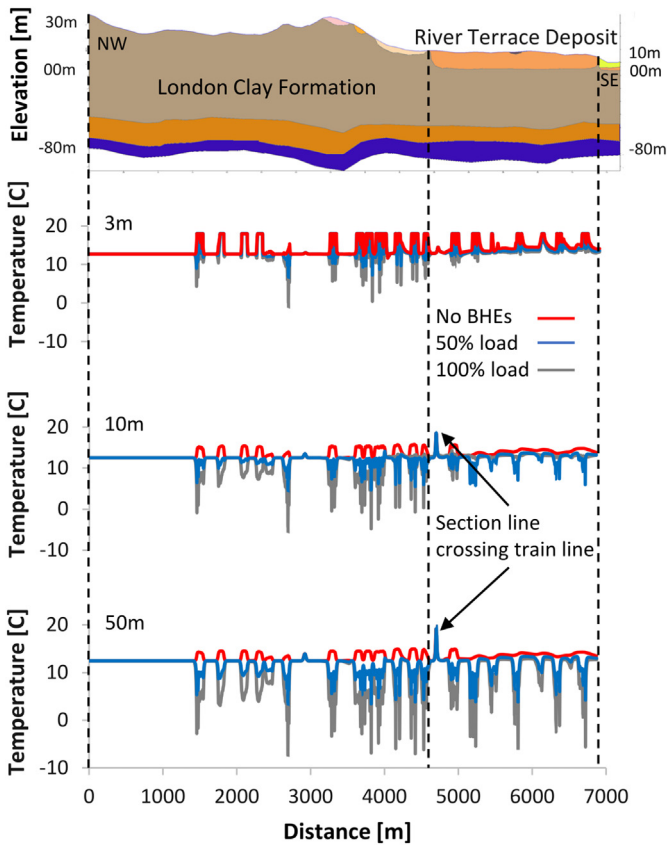

Fig. 8. The ground temperature along NW-SE section at different depths.

for 50% thermal load has resulted from the section line crossing the train tunnels.

In this study, borehole heat exchangers are modelled as point heat sinks, for which their accumulative effect along the depth resembles a line heat source. In general, the efficiency of geothermal systems is evaluated by the temperature of carrier fluid circulating within the BHEs, which is recommended by ground source heat pump manufacturers to be kept at a temperature not lower than 1–2 °C below zero (Bidarmaghz and Narsilio, 2016; Bidarmaghz et al., 2016). The threshold for the ground temperature to prevent ground freezing is, however, 0 °C, which is used in this study. To further evaluate the geothermal potential of the subsurface, in addition to the spatial variations of the ground temperature due to heat extraction, investigating the temperature ranges occurring at point heat sinks provides further insight into the efficiency of geothermal systems in different areas. This is indicated by a percentage of ground heat exchangers that have the temperature sub-zero.

Fig. 9 shows depth-averaged temperatures of point heat sinks for different geological makeup and different thermal load intensities. Even though the number of borehole heat exchangers in different geologies are different (1280 BHEs in an area with River Terrace Deposits underlain by London Clay and 3300 BHEs in the area where London Clay outcrops), the BHEs density (BHE/m^2) is the same in all selected areas. It is observed that the application of geothermal systems to fulfil a given thermal load may not be feasible in a formation such as clay. For example, to fulfil 75% of the total thermal demand via BHEs, 78% of the borehole heat exchangers in that area (out of 3300) reach an average minimum temperature of 0 °C and lower (Fig. 9a), while the rest show above-zero temperatures. This is likely attributed to the configuration of the basements and ground heat exchangers. However, the same thermal demand could be satisfied via the majority of borehole heat exchangers activated in geological units such as sand and gravel, from which around 85% of them show temperatures higher than the threshold (>0 °C - Fig. 9b). The effect of geological makeup is less significant for less intense thermal load distributions.

The supply of 50% of the total thermal demand in the modelled district via borehole heat exchangers is viable because the minimum temperature within almost all the heat sinks at any other point within the ground is higher than the temperature threshold (0 °C) (Fig. 9c and d). That is, up to 50% of the total thermal demand could be supplied by geothermal extraction systems in the entire borough regardless of the geology and hydrogeology. This translates to 33% reduction in CO2 emission when ground source heat pump systems supply 50% of the borough's total gas demand compared to gas use for 100% of the thermal demand. The CO2 reduction calculations are based on London's 2019 emission factors for gas (0.184 $kgCO_2e$/kWh) and electricity (0.253 $kgCO_2e$/kWh) and a typical Coefficient of Performance (COP) of 4 for the ground source heat pump (London Energy and Greenhouse Gas Inventory, 2019; Aditya et al., 2020; Aditya and Narsilio, 2020). In particular, in parts of the borough where River Terrace Deposits outcrops, up to 75% of the thermal demand could be satisfied using the proposed district-scale GSHP systems. For an average gas consumption of 12,500 kWh per household, assuming 0.253 kgCO2e/kWh for electricity and 0.184 kgCO2e/kWh for gas (as per 2019 emission factors for London), the supply of 50% of the total gas demand by ground source heat pump system with a typical COP of 4, results in 33% saving in CO2 emission.

4. Conclusions

This paper investigates the geothermal potential in a densely populated district in London, UK. Using a semi-3D finite element methodology, the spatio-temporal variability of ground temperatures resulting from concurrent thermal interaction between underground heated structures, geothermal installations and the ground is investigated. The hydrogeological variations coupled with the continuous heat rejection from underground spaces has led to a spatial dependency of geothermal potential

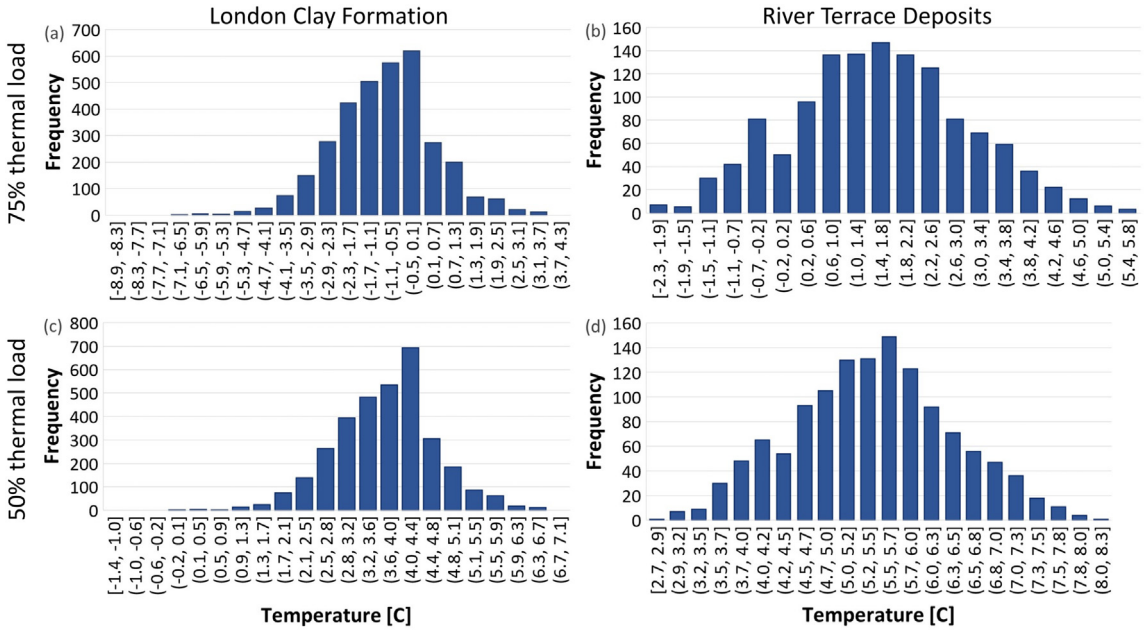

Fig. 9. Ground heat exchangers' temperature range activated at London Clay Formation and River Terrace Deposits for satisfying 75% and 50% of the total thermal demand.

in the district, hence also resulting in the variation of geothermal energy extraction efficiency in different parts of the district.

It is concluded that the shallow subsurface can supply a significant portion of the total energy demand of the district. Temperature distributions at and around borehole heat exchangers show that even though the 100% of the thermal demand cannot be fulfilled by the defined geothermal systems, up to 75% of thermal demand could be supplied using borehole heat exchangers in parts of the district that River Terrace Deposits outcrops. In addition, up to 50% of the total thermal demand could be supplied by geothermal extraction systems in the entire district consisting of sand and gravel in southern parts and clay in the northern parts. This translates to 33% reduction in CO2 emission when ground source heat pump systems supply 50% of the borough's total gas demand compared to gas use for 100% of the thermal demand.

The numerical results show that, although heated underground spaces increase the ground temperature and significantly contribute to its geothermal potential, the high permeability of the ground and groundwater flow are the necessary contributors with respect to the efficiency of geothermal extraction. This highlights the crucial impact of convective heat transfer in urban geothermal potential evaluations. Such hydro-geological characteristics (sand and gravel with groundwater flow) combined with the temperature elevation in the urban underground can result in conditions in which a significant portion (i.e., 75% in this study) of the city's thermal demand can be satisfied via the ground heat exchanger. In the London Clay Formation with low permeability, while the efficiency of geothermal extraction is improved by the heat rejected from underground spaces, its efficiency deviates significantly from the one in sand and gravel formations. Conductive heat transfer is the main heat exchange mechanism in this hydro-geological condition. With underground heat sources being the only contributors to the ground thermal recharge in this formation, the urban geothermal potential is mainly dependent on ground thermal capacities (thermal diffusivity).

The case study illustrates that sustainable application of geothermal systems requires i) detailed knowledge of spatial variations of the ground temperature, ii) hydro-geological properties of the ground and iii) underground built environment characteristics. Once these are known, studying the long-term thermal interactions between the ground, underground heat sources and the borehole heat exchangers and the consequent spatial variations of ground temperature can be conducted for a better estimation of geothermal potential than before. The presented modelling framework can fully capture such thermal interactions on a large scale. Further research work is needed to examine the scalability of the framework by applying it to other subsurface conditions and underground built environment characteristics.

CRediT authorship contribution statement

Asal Bidarmaghz: Formal analysis, Visualization, Writing – original draft, Validation, Methodology. **Ruchi Choudhary:** Conceptualization, Writing – review & editing. **Guillermo Narsilio:** Conceptualization, Writing – review & editing. **Kenichi Soga:** Conceptualization, Writing – review & editing.

Declaration of competing interest

The authors declare that they have no known competing financial interests or personal relationships that could have appeared to influence the work reported in this paper.

Acknowledgements

This work was supported by AI for Science and Government (ASG), UKRI's Strategic Priorities Fund awarded to the Alan Turing Institute, UK and the Lloyd's Register Foundation programme on Data-centric engineering and the NSF-CMMI-EPSRC grant (joint between UC Berkeley and Cambridge University) on “Modelling and monitoring of urban underground climate change”. This material is based upon work supported by the National Science Foundation under Grant No. 1903296 and by EPSRC under Grant No. G103077.

References

Aditya, G.R., Narsilio, G.A., 2020. Environmental assessment of hybrid ground source heat pump systems. Geothermics 87, 101868.

Aditya, G.R., Mikhaylova, O., et al., 2020. Comparative costs of ground source heat pump systems against other forms of heating and cooling for different climatic conditions. Sustain. Energ. Technol. Assess. 4.

Allen, A., Milenic, D., et al., 2003. Shallow gravel aquifers and the urban heat island effect: a source of low enthalpy geothermal energy. Geothermics 32, 569–578.

Anderson, A., Rezaie, B., 2019. Geothermal technology: trends and potential role in a sustainable future. Appl. Energy 248, 18–34.
Arola, T., Korkka-Niemi, K., 2014. The effect of urban heat islands on geothermal potential: examples from quaternary aquifers in Finland. Hydrogeol. J. 22, 1953–1967.
Baggs, S.A., 1983. Remote prediction of ground temperature in Australian soils and mapping its distribution. Sol. Energy 30, 351–366.
Banks, D., 2012. An Introduction to Thermogeology: Ground Source Heating and Cooling. John Wiley & Sons.
Barla, M., Di Donna, A., 2018. Energy tunnels: concept and design aspects. Underground Space 3, 268–276.
Bayer, P., Attard, G., et al., 2019. The geothermal potential of cities. Renew. Sust. Energ. Rev. 106, 17–30.
Bidarmaghz, A., 2014. 3D numerical modelling of vertical ground heat exchangers. PhD Thesis. The University of Melbourne.
Bidarmaghz, A., Narsilio, G., 2016. Shallow geothermal energy emerging convective phenomena in permeable saturated soils. Geotechnique Letters 6, 119–123.
Bidarmaghz, A., Narsilio, G., 2018. Heat exchange mechanisms in energy tunnel systems. Geomechanics for Energy and the Environment.
Bidarmaghz, A., Makasis, N., et al., 2015. Geothermal energy in loess. Environ. Geotech. 3, 225–236.
Bidarmaghz, A., Narsilio, G., et al., 2016. The importance of surface air temperature fluctuations on long-term performance of vertical ground heat exchangers. Geomech. Energ. Environ. 6, 35–44.
Bidarmaghz, A., Narsilio, G., et al., 2017. Thermal interaction between tunnel ground heat exchangers and borehole heat exchangers. Geomech. Energ. Environ. 10, 29–41.
Bidarmaghz, A., Choudhary, R., et al., 2019. Influence of geology and hydrogeology on heat rejection from residential basements in urban areas. Tunn. Undergr. Space Technol. 92.
Bidarmaghz, A., Choudhary, R., et al., 2020. Large-scale urban underground hydro-thermal modelling – a case study of the Royal Borough of Kensington and Chelsea, London. Sci. Total Environ. 700.
Bricker, S., Bloomfield, J., 2014. Controls on the basin-scale distribution of hydraulic conductivity of superficial deposits: a case study from the Thames Basin, UK. Q. J. Eng. Geol. Hydrogeol. 47, 223–236.
British Geological Survey, 2017. RE: Ground Thermal and Hydraulic Property Data.
Burke, H., Mathers, S., et al., 2014. The London Basin Superficial and Bedrock LithoFrame 50 Model.
Busby, J., Lewis, M., et al., 2009. Initial geological considerations before installing ground source heat pump systems. Q. J. Eng. Geol. Hydrogeol. 42, 295–306.
Choudhary, R., 2012. Energy analysis of the non-domestic building stock of greater London. Build. Environ. 51, 243–254.
COMSOL. 2018a. *Heat Transfer Module User's Guide* [Online].
COMSOL. 2018b. *Subsurface Flow Module User's Guide* [Online].
Cousin, B., Loria, A.F.R., et al., 2018. Feasibility and Energy Performance of an Energy Segmental Lining for a Subway Tunnel.
Epting, J., García-Gil, A., et al. 2017. Development of concepts for the management of thermal resources in urban areas–assessment of transferability from the Basel (Switzerland) and Zaragoza (Spain) case studies. 548, 697–715.
Epting, J., Müller, M.H., et al., 2018. Relating groundwater heat-potential to city-scale heat-demand: a theoretical consideration for urban groundwater resource management. Appl. Energy 228, 1499–1505.
Epting, J., Baralis, M., et al., 2020. Geothermal potential of tunnel infrastructures–development of tools at the city-scale of Basel, Switzerland. Geothermics 83, 101734.
Ferguson, G., Woodbury, A.D., 2004. Subsurface heat flow in an urban environment. J. Geophys. Res. 109.
GeoInformation, 2017a. UK buildings. Analytics V. (Ed.) 5 ed. UK.
GeoInformation, 2017b. UK map. Analytics (V. (Ed.). UK).
Gilbey, M., Duffy, S., et al., 2011. The Potential for Heat Recovery from London Underground Stations and Tunnels. DeMontfort University, Proceedings of CIBSE technology and symposium.
Johnston, I., Narsilio, G., et al., 2011. Emerging geothermal energy technologies. KSCE J. Civ. Eng. 15, 643–653.
Kavanaugh, S.P., Rafferty, K.D., 2014. Geothermal Heating and Cooling: Design of Ground-Source Heat Pump Systems. ASHRAE.
Lane, M., 2011. How Warm Is your Home. BBC Magazine, UK.
London Energy and Greenhouse Gas Inventory. 2019.
Mansour, M., Hughes, A.G., 2004. User's Manual for the Distributed Recharge Model ZOODRM.
Mansour, M., Wang, L., et al., 2018. Estimation of spatially distributed groundwater potential recharge for the United Kingdom. Q. J. Eng. Geol. Hydrogeol. 51, 247–263.
Menberg, K., Heo, Y., et al., 2016. Sensitivity analysis methods for building energy models: comparing computational costs and extractable information. Energ. Build. 133, 433–445.
Meng, B., Vienken, T., et al., 2019. Evaluating the thermal impacts and sustainability of intensive shallow geothermal utilisation on a neighborhood scale: lessons learned from a case study. Energy Convers. Manag. 199, 111913.
Mortada, A., 2019. Energy Efficient Passenger Comfort in Underground Subway Environments. University of Cambridge.
Ondreka, J., Rüsgen, M.I., et al., 2007. GIS-supported mapping of shallow geothermal potential of representative areas in South-Western Germany—possibilities and limitations. Renew. Energy 32, 2186–2200.
Østergaard, P.A., Lund, H., 2011. A renewable energy system in Frederikshavn using low-temperature geothermal energy for district heating. Appl. Energy 88, 479–487.
Price, S.J., Terrington, R.L., et al., 2018. 3D ground-use optimisation for sustainable urban development planning: a case-study from earls court, London, UK. Tunn. Undergr. Space Technol. 81, 144–164.
Radioti, G., Sartor, K., et al., 2017. Effect of undisturbed ground temperature on the design of closed-loop geothermal systems: a case study in a semi-urban environment. Appl. Energy 200, 89–105.
RBKC, 2018. Planning and Building Control Portal/Planning Search.
Rivera, J.A., Blum, P., et al., 2017. Increased ground temperatures in urban areas: estimation of the technical geothermal potential. Renew. Energy 103, 388–400.
Taniguchi, M., Shimada, J., et al., 2009. Anthropogenic effects on the subsurface thermal and groundwater environments. Sci. Total Environ. 407, 3153–3164.
Todd, D.K., 1959. Ground Water Hydrology. John Wiley and Sons, Inc, New York.
Vienken, T., Kreck, M., et al., 2019. Monitoring the impact of intensive shallow geothermal energy use on groundwater temperatures in a residential neighborhood. Geotherm. Energ. 7, 1–14.
Zhang, Y., Soga, K., et al., 2014. Shallow geothermal energy application with GSHPs at city scale: study on the city of Westminster. Géotechnique Lett. 4, 125–131.
Zimmermann, J.-P., Evans, M., et al., 2012. Household Electricity Survey: A Study of Domestic Electrical Product Usage.